SECURITY CLASSIFICATION OF THIS PAGE

REPORT DOCUMENTATION PAGE

Form Approved OMB No 0704 0188

AD-A237 509

1a. R

2a. S

2b. DECLASSIFICATION/DOWNGRADING SCHEDULE

1b. RESTRICTIVE MARKINGS

3. DISTRIBUTION/AVAILABILITY OF REPORT
Approved for public release and sale; its distribution is unlimited.

4. PERFORMING ORGANIZATION REPORT NUMBER(S)
Technical Report No. 107

5. MONITORING ORGANIZATION REPORT NUMBER(S)

6a. NAME OF PERFORMING ORGANIZATION
Purdue University
Department of Chemistry

6b. OFFICE SYMBOL (If applicable)

7a. NAME OF MONITORING ORGANIZATION
Division of Sponsored Programs
Purdue Research Foundation

6c. ADDRESS (City, State, and ZIP Code)
Purdue University
Department of Chemistry
West Lafayette, IN 47907

7b. ADDRESS (City, State, and ZIP Code)
Purdue University
West Lafayette, IN 47907

8a. NAME OF FUNDING/SPONSORING ORGANIZATION
Office of Naval Research

8b. OFFICE SYMBOL (If applicable)

9. PROCUREMENT INSTRUMENT IDENTIFICATION NUMBER
Contract No. N00014-91-J-1409

8c. ADDRESS (City, State, and ZIP Code)
800 N. Quincy Street
Arlington, VA 22217

10. SOURCE OF FUNDING NUMBERS

PROGRAM ELEMENT NO.	PROJECT NO.	TASK NO	WORK UNIT ACCESSION NO

11. TITLE (Include Security Classification)
The Influence of Potential on Metal-Adsorbate Structure: Solvent-Independent Nature of Infrared Spectra for Pt(111)/CO

12. PERSONAL AUTHOR(S)
S.-C. Chang, X. Jiang, J.D. Roth, and M.J. Weaver

13a. TYPE OF REPORT
Technical

13b. TIME COVERED
FROM _____ TO _____

14. DATE OF REPORT (Year, Month, Day)
May 31, 1991

15. PAGE COUNT

16. SUPPLEMENTARY NOTATION

17. COSATI CODES

FIELD	GROUP	SUB-GROUP

18. SUBJECT TERMS (Continue on reverse if necessary and identify by block number)
in-situ infrared spectra in C-O stretching region, aqueous electrochemical and ultrahigh vacuum environments, surface potential drop

19. ABSTRACT (Continue on reverse if necessary and identify by block number)

In-situ infrared spectra are reported in the C-O stretching (ν_{co}) region for saturated CO adlayers on Pt(111) in four nonaqueous solvents; acetonitrile, dimethylformamide, dichloromethane and tetrahydrofuran, each containing tetraalkylammonium cations, over wide electrode potential ranges, ca -2.0 to 1.5 V vs SCE. Notably, the spectral features (ν_{co} frequencies, CO site occupancies, etc) are sensitive only to the applied potential, being virtually independent of the solvating medium. Comparisons with spectra obtained in the presence of different cations, and in corresponding aqueous electrochemical and ultrahigh vacuum environments, demonstrate that the adlayer properties are controlled in each case by the surface potential drop across the adsorbate layer.

20. DISTRIBUTION/AVAILABILITY OF ABSTRACT
☐ UNCLASSIFIED/UNLIMITED ☐ SAME AS RPT. ☐ DTIC USERS

21. ABSTRACT SECURITY CLASSIFICATION

22a. NAME OF RESPONSIBLE INDIVIDUAL

22b. TELEPHONE (Include Area Code)

22c. OFFICE SYMBOL

DD Form 1473, JUN 86 Previous editions are obsolete. SECURITY CLASSIFICATION OF THIS PAGE

OFFICE OF NAVAL RESEARCH

Contract No. N00014-91-J-1409

Technical Report No. 107

The Influence of Potential on Metal-Adsorbate Structure: Solvent-Independent Nature of Infrared Spectra for Pt(111)/CO

by

S.-C. Chang, X. Jiang, J.D. Roth, and M.J. Weaver

Prepared for Publication

in the

Journal of Physical Chemistry

Purdue Univeristy

Department of Chemistry

West Lafayette, Indiana 47907

May 1991

The Influence of Potential on Metal-Adsorbate Structure: Solvent-Independent Nature of Infrared Spectra for Pt(111)/CO

Si-Chung Chang, Xudong Jiang, Joseph D. Roth
and Michael J. Weaver*

Department of Chemistry, Purdue University
West Lafayette, Indiana 47907

J. Phys. Chem. (Letter)
submitted April 12, 1991
revised May 17, 1991

ABSTRACT

In-situ infrared spectra are reported in the C-O stretching (ν_{co}) region for saturated CO adlayers on Pt(111) in four nonaqueous solvents; acetonitrile, dimethylformamide, dichloromethane and tetrahydrofuran, each containing tetraalkylammonium cations, over wide electrode potential ranges, ca -2.0 to 1.5 V vs SCE. Notably, the spectral features (ν_{co} frequencies, CO site occupancies, etc) are sensitive only to the applied potential, being virtually independent of the solvating medium. Comparisons with spectra obtained in the presence of different cations, and in corresponding aqueous electrochemical and ultrahigh vacuum environments, demonstrate that the adlayer properties are controlled in each case by the surface potential drop across the adsorbate layer.

A fundamental topic in electrochemical surface science concerns the manner and extent to which the adsorbate bonding and adlayer structure is influenced by the applied potential. Although not always recognized as such, this issue is also of relevance to adsorption at metal-ultrahigh vacuum (uhv) interfaces, especially in the presence of ionizable and strongly dipolar coadsorbates. The recent development of infrared reflection-absorption spectroscopy (IRAS) for the in-situ examination of ordered monocrystalline metal-solution interfaces is enabling molecular-level information on adsorbate structure to be obtained in a manner previously exclusive to uhv surface science. The adsorption of carbon monoxide is of particular interest in this regard, given the sensitivity of the C-O vibration (ν_{co}) to the details of surface bonding.

We have recently undertaken a series of in-situ IRAS studies of the adsorption and electrooxidation of CO at ordered low-index platinum and rhodium surfaces in aqueous media.[1-6] One important aspect involves comparisons of the ν_{co} frequencies and adsorbate coordination geometry at metal-solution interfaces with the corresponding metal-uhv surfaces.[1,5] Intriguingly, the often marked dissimilarities observed in the adlayer spectral properties can be accounted for at least partly in terms of the substantial differences in surface potential between the aqueous electrochemical and uhv environments. A limitation of aqueous media for these purposes is that the occurrence of CO electrooxidation restricts the range of electrochemical surface potentials to values substantially (ca 0.5 - 1 V) below those encountered at the metal-uhv interfaces.[1] This difficulty can be circumvented by the use of nonaqueous solvents. Such media often provide a much wider range of potentials in the negative as well as positive directions, and enable the possible occurrence of specific solvent effects on the adlayer structure to be explored. So far, however, reports of infrared spectra for CO at metal-nonaqueous interfaces have been sparse and

limited to polycrystalline materials.[6c,7]

Reported here are potential-dependent infrared spectra for saturated CO adlayers on ordered Pt(111) in four nonaqueous solvents: acetonitrile, dimethylformamide (DMF), dichloromethane, and tetrahydrofuran (THF), as well as water. These media span a wide range of dielectric and solvating properties. Nevertheless, the potential-dependent ν_{co} frequencies and site occupancies display a remarkable insensitivity to the solvating medium in the presence of a given supporting electrolyte cation. The data also allow a direct comparison to be made between the CO spectral properties on Pt(111) in these nonaqueous electrochemical environments with corresponding uhv results *at the same surface potential*, enabling the role of the double layer on the adlayer structure to be further delineated.

EXPERIMENTAL

Details of the electrochemical IRAS measurements are largely as provided in refs. 3a and 8. The infrared spectrometer was an IBM (Bruker) IR-98-4A Fourier transform instrument, with a Globar light source and a liquid-N_2 cooled MCT detector (Infrared Associates). The Pt(111) crystal (9 mm diameter, 4 mm thick) was purchased from the Material Preparation Facility at Cornell University. It was oriented within ±1°, as verified by x-ray diffraction. The surface pretreatment procedures, including hydrogen-air flame annealing, gas-phase iodine adsorption during cooling, and subsequent replacement with adsorbed CO in 0.1 M $HClO_4$, are described in ref. 2a. After removal of the irreversibly adsorbed CO in turn by a 50 mV s^{-1} positive-going voltammetric sweep (to 0.6 vs SCE), the crystal (mounted on a glass plunger) was thoroughly rinsed with the desired solvent and immediately transferred to the infrared cell containing the same solvent saturated with CO. Acetonitrile, THF, and dichloromethane were

purified prior to use by distillation from the appropriate desiccant (calcium hydride, sodium metal, and P_2O_5, respectively) under dry N_2. The dimethylformamide (Burdick and Jackson) was used as received. The tetrabutylammonium perchlorate (TBAP) and tetraethylammonium perchlorate (TEAP) used as supporting electrolytes were recrystallized from methanol, and from water and ethanol, respectively, and dried under vacuum at 110°C. Electrode potentials were measured versus the ferrocenium-ferrocene (Fc^+/Fc) couple in the same solvent/supporting electrolyte; this involved the use of an equimolar Fc^+/Fc mixture in contact with a Pt wire in a separate reference compartment. The electrode potentials quoted here in each solvent, however, are versus an aqueous saturated calomel electrode with a solvent liquid junction formed in the presence of 0.1 M TEAP. This approach yields more reliable comparative electrode potentials in different solvents than by using the Fc^+/Fc reference electrode scale (vide infra).[9]

RESULTS

After transferring the Pt(111) surface to the CO-saturated nonaqueous medium and forming the spectral thin layer, sequences of ν_{co} spectra were recorded over the range of electrode potentials bound by the onset of electrochemical reduction and oxidation. As usual,[3,8b] potential-difference infrared spectra were obtained by subtracting pairs of interferometer scans acquired at suitably disparate "sample" and "reference" electrode potentials (E_S and E_R), so to remove the solvent interference. An especially useful tactic involves acquiring sets of 100 interferometer scans during a slow (2 mV s^{-1}) positive-going potential sweep. Representative spectra obtained in this fashion in CO-saturated acetonitrile containing 0.15 M TBAP, starting at -1.6 V vs SCE, are shown in Fig. 1. In this example, traces of water resulted in the electrooxidative removal of adsorbed CO at ca 1.0 V. Using a reference spectrum acquired

at the latter potential (E_R) to subtract from the preceding interferometer scans therefore enabled absolute (i.e., unipolar) ν_{co} absorbance spectra to be obtained, as displayed in Fig. 1. In the absence of water, CO electrooxidation did not proceed even at higher potentials. (At such high potentials in the presence of water, CO electrooxidation probably resulted in surface disordering.[2a]) While bipolar ν_{co} bands, reflecting the spectral components at E_S and E_R, are necessarily obtained under the latter circumstances, for well-separated E_S/E_R combinations these ν_{co} peaks occur at sufficiently different frequencies so that their mutual interference is small or negligible.

A pair of ν_{co} bands are observed in Fig. 1: a major feature at ca 2050 to 2100 cm^{-1}, and a weaker component at ca 1770-1870 cm^{-1}. As usual, the ν_{co} frequencies upshift monotonically with increasing electrode potential. The form of these spectra is very similar to those obtained for saturated CO layers in CO-saturated aqueous acidic media (see Fig. 1 of ref. 5). By analogy with uhv spectra and other evidence, the intense high-frequency feature can be ascribed to atop (i.e., terminal), or near-atop, CO coordination.[5] The low-frequency band observed at potentials below 0.2 V in Fig. 1, also seen in aqueous media, has been ascribed to CO bound to threefold hollow sites.[5] The sharp replacement of this band by a similar feature at ca 45 cm^{-1} higher frequencies for $E > 0.2$ V is suggestive of an adlayer structural change whereby twofold bridging CO is formed.[5]

Remarkably similar potential-dependent spectral features were observed over the potential range ca -2 to 1.5 V vs SCE in the other three nonaqueous solvents examined here. Plots of the peak frequency of the terminal band, ν^t_{co}, as a function of electrode potential, E, in the four nonaqueous solvents containing 0.15 M TBAP are shown in Fig. 2. The corresponding plots of the multifold (bridging) band frequency, ν^b_{co}, against E are displayed in Fig. 3 (see captions

for solvent identification). The ν^t_{co} or ν^b_{co} values at a given potential are seen to differ by 2–3 cm^{-1} or less between these solvents throughout the entire ca 3 V potential range. Indeed, some of these minor differences may result from uncertainties in the metal–solution potential scale as the solvent is varied. Moreover, the transition between the two CO adlayer structures, as discerned from the sharp change in ν^b_{co}, occurs at virtually the same electrode potential, 0 to 0.05 V vs SCE, in all four solvents. Additional manifestations of this adlayer structural change are the noticeably (ca 30%) larger ν^t_{co}– E slopes observed at potentials above the transition (Fig. 2), and a slight diminution in the terminal bandwidth along with an increase in the peak height (Fig. 1).

Quantitative determination of the CO coverage, θ_{co}, is precluded, at least using the spectrophotometric and faradaic assay of electrooxidation to CO_2 employed in aqueous media.[2] Nevertheless, the formation of uniformly high, essentially saturated, CO coverages (θ^{sat}_{co}) with $\theta_{co} \approx 0.6$–0.7,[2a] is inferred by the near-constant (±10%) integrated absorbance values, A^t_i, for the dominant terminal ν_{co} feature in the various media considered here (Table I).

Significantly different behavior was induced, however, by altering the supporting electrolyte cation. These experiments were motivated originally by the desire to employ a cation, tetraethylammonium (TEA^+), that is suitably soluble in water as well as nonaqueous media. The ν^t_{co}– E data obtained in acetonitrile containing 0.15 M TEAP (open squares) and 0.15 M TBAP (open circles), and in aqueous 0.15 M TEAP (filled squares) are compared in Fig. 4. The corresponding ν^b_{co}– E data are shown in Fig. 5. (This supporting electrolyte comparison was limited to acetonitrile by solubility considerations.) The substitution of TBA^+ by TEA^+ is seen to yield significantly divergent behavior, larger ν^t_{co}– E and ν^b_{co}– E slopes being obtained with the latter cation (Figs. 4,5). Nevertheless, the ν^t_{co}– E plots in acetonitrile and water containing TEAP are

almost coincident (Fig. 4), again affirming the lack of a significant solvent effect upon the spectral properties in a given supporting electrolyte. This close similarity is also reflected in a near-coincidence of the transition potential at which the adlayer structure occurs in these media (Fig. 5). For comparison, ν^{t}_{co}– E and ν^{b}_{co}– E data (taken from ref. 5) are also shown in aqueous 0.1 M $HClO_4$ (filled triangles, Figs. 4, 5); this electrolyte has been used extensively in our aqueous-based studies.[2-6] Spectra were also obtained in acetonitrile and THF containing 0.15 M $NaClO_4$. In contrast to the corresponding data with 0.15 M TBAP, the terminal band is replaced at negative potentials (beyond ca –0.5 V) by weaker features at lower frequencies, 1650–1800 cm^{-1}. The observed behavior is similar to that obtained with polycrystalline platinum,[6c] and is consistent with specific cation-induced CO site conversion.

A summary of some relevant infrared band parameters, specifically ν_{co}– E slopes, A_1 values, and bandwidths ($\Delta\nu_{1/2}$), in the various media examined here are summarized in Table I. In most cases, the data are quoted at a pair of potentials, –1.0 and 0.5 V vs SCE, corresponding to the occurrence of the "low-" and "high-potential" adlayer structures, respectively.

DISCUSSION

The present results indicate that the solvent exerts remarkably little (or conceivably a near-invariant) influence on the spectral properties of the Pt(111)/CO(θ^{sat}_{co}) interface at a given applied electrode potential E. To an acceptable approximation (say within ca 0.1 V), a given E value in different solvents implies a near-constant metal-solution potential difference ϕ_{M-S}. One can therefore infer that the adlayer properties of this system are controlled chiefly by ϕ_{M-S} rather than by the specific solvating environment. While expected to be a general property of CO adlayers only at saturated coverages, this simple result probably arises from the exclusion of solvent molecules from

the electrochemical inner layer, the solvent merely acting as the dispersing medium with'n which the ionic component of the double layer is located.

Given this situation, it is profitable to compare the spectral properties of the Pt(111)/CO electrochemical interface with the corresponding uhv system at the same surface potential ϕ_M. From work-function data, the ϕ_M value for the latter (uncharged) interface is about 1.0 V on the SCE scale.[10] At this potential at the Pt(111)-nonaqueous interfaces, ν^t_{co} values of 2091-2094 cm^{-1} are observed (Fig. 2). Precise comparison with ν^t_{co} for the Pt(111)-uhv system is hampered by the inability to attain compressed CO adlayers at ambient temperatures. However, a similar ν^t_{co} value, ca 2095 cm^{-1}, for Pt(111)/CO($\theta_{co} \approx 0.6$-0.7) at 300K can be deduced from data in ref. 11. The corresponding frequency comparison for the bridging ν_{co} feature is complicated by the observed coverage-sensitivity of ν^b_{co} at high θ_{co} in the uhv system.[11b] Nevertheless, the observed electrochemical ν^b_{co} value at 1.0 V vs SCE, 1865-1875 cm^{-1} (Fig. 3), is comparable to (within ca 15 cm^{-1} of) those obtained for the uhv system.[11b] The ratio of integrated absorbances (A^t_I/A^b_I) of the terminal and bridging features in the Pt(111)-uhv system, ca 6, is also roughly comparable to those observed for the electrochemical interfaces, ca 5-7, at 1.0 V (Table I). The bandwidths of the terminal ν_{co} feature at the Pt(111)-solution interfaces, 11-14 cm^{-1} (Table I), are nonetheless significantly larger than that obtained, ca 7 cm^{-1}, for the uhv system at 300K.[11a] This difference most likely results from line-broadening effects associated with local solvation.

The effect of varying the supporting-electrolyte cation, most simply TBA^+ versus TEA^+ in acetonitrile (Fig. 4), can be understood in terms of a simple double-layer model. In the expected absence of a marked net orientation of interfacial solvent dipoles in the presence of saturated CO adlayers, the potential of zero charge (E_{pzc}) of the Pt(111)/CO - nonaqueous interfaces should

be close to that for the corresponding uhv surface, 1.0 V vs. SCE, since the latter interface is necessarily uncharged. To the extent that the observed spectral differences between TBA^+ and TEA^+ are due to variations in electrostatic field, this cation effect should eventually disappear at E_{pzc}, by ca 1.0 V.

Inspection of Fig. 4 shows that this is indeed the case. Moreover, the progressively greater ν^t_{co} discrimination observed in TBA^+ and TEA^+ as the potential decreases below 1.0 V, i.e. the dissimilarities in the ν^t_{co}–E slopes (Fig. 4, Table I), can be understood simply in terms of the differences in average electrostatic field resulting from the unequal crystallographic radii, r_c, of TBA^+ (4.95 Å) and TEA^+ (4.0 Å).[12] This field is induced by the negative electrode charge and accompanying cationic charge, located largely at the outer Helmholtz plane (oHp). We take the "thickness" of the CO adlayer, d_{co}, to be 3.1 Å[13], and assume the oHp is located at a distance (d_{co} + r_c) from the metal surface. If the electrostatic field is constant across this inner layer, and the CO molecules sense only the portion of the potential drop, then the variation of $d\nu^t_{co}/dE$ with the electrolyte cation will be proportional to $(d_{co} + r_c)^{-1}$.

The ratio of $d\nu_{co}/dE$ values for TEA^+ versus TBA^+ predicted on this basis, 1.13, is in reasonable accordance with the experimental $d\nu^t_{co}/dE$ ratios in acetonitrile, 1.1 to 1.15 (Table I). The same argument can account semiquantitatively for the larger $d\nu^t_{co}/dE$ values observed in water containing $HClO_4$ versus TEAP electrolytes (Fig. 4), given the smaller hydrated radius of H_3O^+.[12] The experimental findings, however, do not impact the much-discussed issue of the relative importance of potential-induced surface-adsorbate charge sharing as distinct from electrostatic-field effects upon the ν_{co} frequencies.[1a,14] Rather, they simply imply that $d\nu_{co}/dE$ (and hence $d\nu_{co}/d\phi_M$) is affected primarily by the component of ϕ_{M-S} lying geometrically within the CO layer.

Overall, then, the present findings provide unexpectedly straightforward

support to the notion, espoused elsewhere[1a], that a major and even predominant effect upon the structure of saturated CO layers is provided by the average surface potential drop. Such infrared spectral measurements for a wider range of ordered metal-nonaqueous-electrolyte systems are currently being pursued in our laboratory.

Acknowledgment

This work is supported by the National Science Foundation and the Office of Naval Research.

REFERENCES AND NOTES

1. For overviews, see: (a) Chang, S.-C.; Weaver, M.J., J. Phys. Chem., in press (Feature Article); (b) Chang, S.-C.; Roth, J.D.; Ho, Y.; Weaver, M.J., J. Electron. Spect. Related Phenom., 1990, 54/55, 1185.

2. (a) Leung, L.-W.H.; Wieckowski, A.; Weaver, M.J., J. Phys. Chem., 1988, 92, 6985; (b) Chang, S.-C.; Leung, L.-W.H.; Weaver, M.J., J. Phys. Chem., 1989, 93, 5341.

3. (a) Chang, S.-C.; Weaver, M.J., J. Chem. Phys., 1990, 92, 4582; (b) Chang, S.-C.; Weaver, M.J., J. Phys. Chem., 1990, 94, 5095; (c) Chang, S.-C.; Weaver, M.J., Surface Sci., 1990, 230, 222.

4. (a) Leung, L.-W.H.; Chang, S.-C.; Weaver, M.J., J. Chem. Phys., 1989, 90, 7426; (b) Chang, S.-C.; Weaver, M.J., J. Electroanal. Chem., 1990, 285, 263.

5. Chang, S.-C.; Weaver, M.J., Surface Sci., 1990, 238, 142.

6. (a) Chang, S.-C.; Weaver, M.J., Surface Sci., 1991, 241, 11; (b) Chang, S.-C.; Roth, J.D.; Weaver, M.J., Surface Sci., 1991, 244, 113; (c) Roth, J.D.; Chang, S.-C.; Weaver, M.J., J. Electroanal. Chem., 1990, 288, 285.

7. (a) Anderson, M.R.; Blackwood, D.; Pons, S., J. Electroanal. Chem., 1988, 256, 387; (b) Anderson, M.R.; Blackwood, D.; Richmond, T.G.; Pons, S., J. Electroanal. Chem., 1988, 256, 397.

8. (a) Corrigan, D.S.; Weaver, M.J., J. Phys. Chem., 1986, 90, 5300;

(b) Corrigan, D.S.; Weaver, M.J., J. Electroanal. Chem., 1988, 241, 143.

9. (a) Sahami, S.; Weaver, M.J., J. Solution Chem., 1981, 10, 199;
(b) Diggle, J.W.; Parker, A.J., Electrochim. Acta., 1973, 18, 975.

10. The "absolute" work function of the Pt(111)/CO(θ_{CO}^{sat})-uhv interface is about 5.9 eV.[3a] Taking the "absolute" potential of the normal hydrogen electrode (NHE) as 4.6 (±0.2)V,[1a] given that the SCE scale is shifted 0.25 V positive vs NHE, the ϕ_M value of this uhv surface is deduced to be 1.05 V vs SCE. (See ref. 3a for discussion of relevant issues.)

11. (a) Schweizer, E.; Persson, B.N.J.; Tüshaus, M.; Hoge, D.; Bradshaw, A.M., Surface Science, 1989, 213, 49; (b) Persson, B.N.J.; Tüshaus, M.; Bradshaw, A.M., J. Chem. Phys., 1990, 92, 5034.

12. For a compilation, see: Nightingale,Jr, E.R., J. Phys. Chem.,1959, 63, 1381.

13. This estimate of d_{CO}, from the edge of the Pt(111) surface plane to the periphery of the CO oxygen atom, is deduced by assuming Pt–C and C–O bond lengths of 1.9 and 1.2 Å, a Pt atomic radius of 1.4 Å, and an oxygen Van der Waals radius of 1.4 Å.

14. For example, see (a) Lambert,D.K., J. Chem. Phys., 1988, 89, 3847., (b) Anderson, A.B., J. Phys. Chem., 1990, 280, 37.

TABLE I Representative infrared ν_{co} data for terminal and bridging CO at Pt(111)-nonaqueous and -aqueous interfaces

Solvents	Electrolyte	Potential V vs SCE	A_i^t [a] cm^{-1}	$\Delta\nu_{1/2}^t$ [b] cm^{-1}	$d\nu_{co}^t/dE$ [c] $cm^{-1}\ V^{-1}$	A_i^b [d] cm^{-1}	$\Delta\nu_{1/2}^b$ [e] cm^{-1}	$d\nu_{co}^b/dE$ [f] $cm^{-1}\ V^{-1}$
CH_3CN	0.15 M TBAP	-1.0	0.11	14	13	0.03	16	20.5
		0.5	0.11	11	20	0.04	18	23.5
	0.15 M TEAP	-1.0	0.11	13	16	0.04	18	20
		0.5	0.11	13	22	0.015	15	21
DMF	0.15 M TBAP	-1.0	0.08	14	13	0.015	16	18
		0.5	0.10	13	13.5	0.015	17	13
CH_2Cl_2	0.15 M TBAP	-1.0	0.11	14	13.5	0.03	16	19
		0.5	0.11	13	19	0.025	19	25
THF	0.15 M TBAP	-1.0	0.10	12	13.5	0.025	20	18.5
		0.5	0.10	11	16.5	0.015	12	16
H_2O	0.10 M $HClO_4$	-0.25	0.10	14	29	0.010	13	58
		0.1	0.11	12	29	0.03	16	46
	0.15 M TEAP	-0.25	0.09	12	18	0.03	16	28
		0.1	0.11	12	18	0.05	16	47

[a] Integrated absorbance of terminal ν_{co} band at electrode potential indicated.

[b] Full width at half maximum absorbance of terminal ν_{co} band.

[c] Slope of ν_{co}^t- E plot at electrode potential indicated at constant site occupancy.

[d] Integrated absorbance of bridging ν_{co} band at electrode potential indicated.

[e] Full width at half maximum absorbance of bridging ν_{co} band.

[f] Slope of ν_{co}^b- E plot at electrode potential indicated at constant site occupancy.

FIGURE CAPTIONS

Fig. 1

Sequences of infrared absorbance spectra in C–O stretching region for adsorbed CO on Pt(111) in CO–saturated acetonitrile containing 0.15 M TBAP obtained during positive-going potential sweep at 2mV s^{-1} from –1.60 V vs SCE. Each spectrum involved acquiring 100 interferometer scans (consuming ca 1min.), subtracted from which was a similar set of scans acquired after complete CO electrooxidation, at ca 1.0 V. Potentials indicated alongside each spectrum are average values (vs SCE) during the spectral acquisition.

Fig. 2

Plots of peak frequency of terminal C–O stretch, ν^t_{co}, versus electrode potential for CO on Pt(111) in CO–saturated solvents as indicated: circles, acetonitrile + 0.15 M TBAP; inverted triangles, DMF + 0.15 M TBAP; upright triangles, dichloromethane + 0.15 M TBAP; squares, THF + 0.15 M TBAP.

Fig. 3

Plots of peak frequency of bridging C–O stretch, ν^b_{co}, versus electrode potential for CO on Pt(111) in CO–saturated solvents as indicated. circles, acetonitrile + 0.15 M TBAP; inverted triangles, DMF + 0.15 M TBAP; upright triangles, dichloromethane + 0.15 M TBAP; squares, THF + 0.15 M TBAP.

Fig. 4

Plots of peak frequency of terminal C–O stretch, ν^t_{co}, versus electrode potential for CO on Pt(111) in CO–saturated solvents as indicated: circles, acetonitrile + 0.15 M TBAP; open squares, acetonitrile + 0.15 M TEAP; filled squares, water + 0.15 M TEAP; filled inverted triangles, water + 0.1 M $HClO_4$.

Fig. 5

Plots of peak frequency of bridging C–O stretch, ν^b_{co}, versus electrode potential for CO on Pt(111) in CO–saturated solvents as indicated. circles, acetonitrile + 0.15 M TBAP; open squares, acetonitrile + 0.15 M TEAP; filled squares, water + 0.15 M TEAP; filled inverted triangles, water + 0.1 M $HClO_4$.

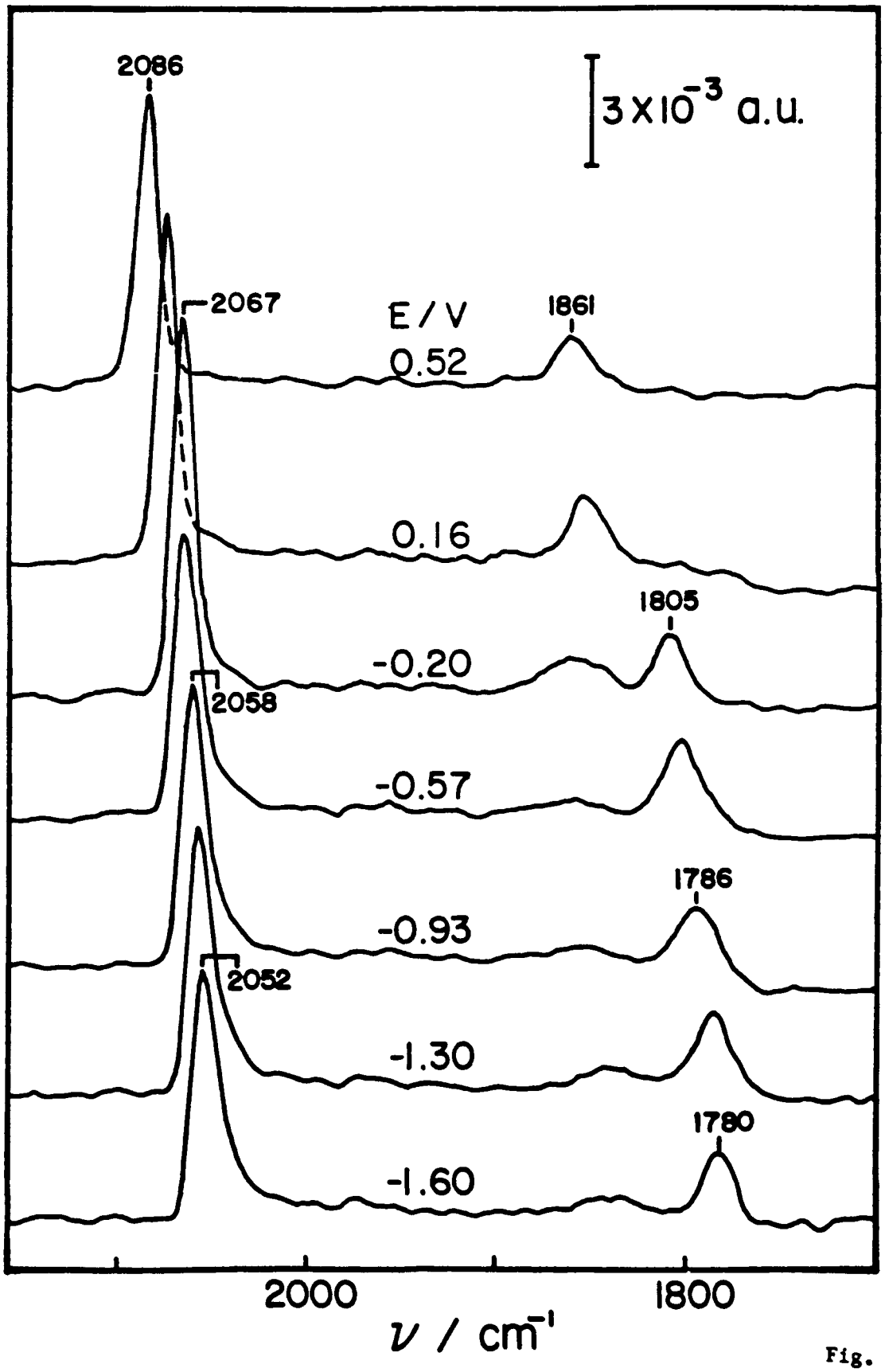
2086
3 X 10⁻³ a.u.
2067
E / V
1861
0.52
0.16
1805
-0.20
2058
-0.57
1786
-0.93
2052
-1.30
1780
-1.60
2000
1800
ν / cm⁻¹

Fig. 1

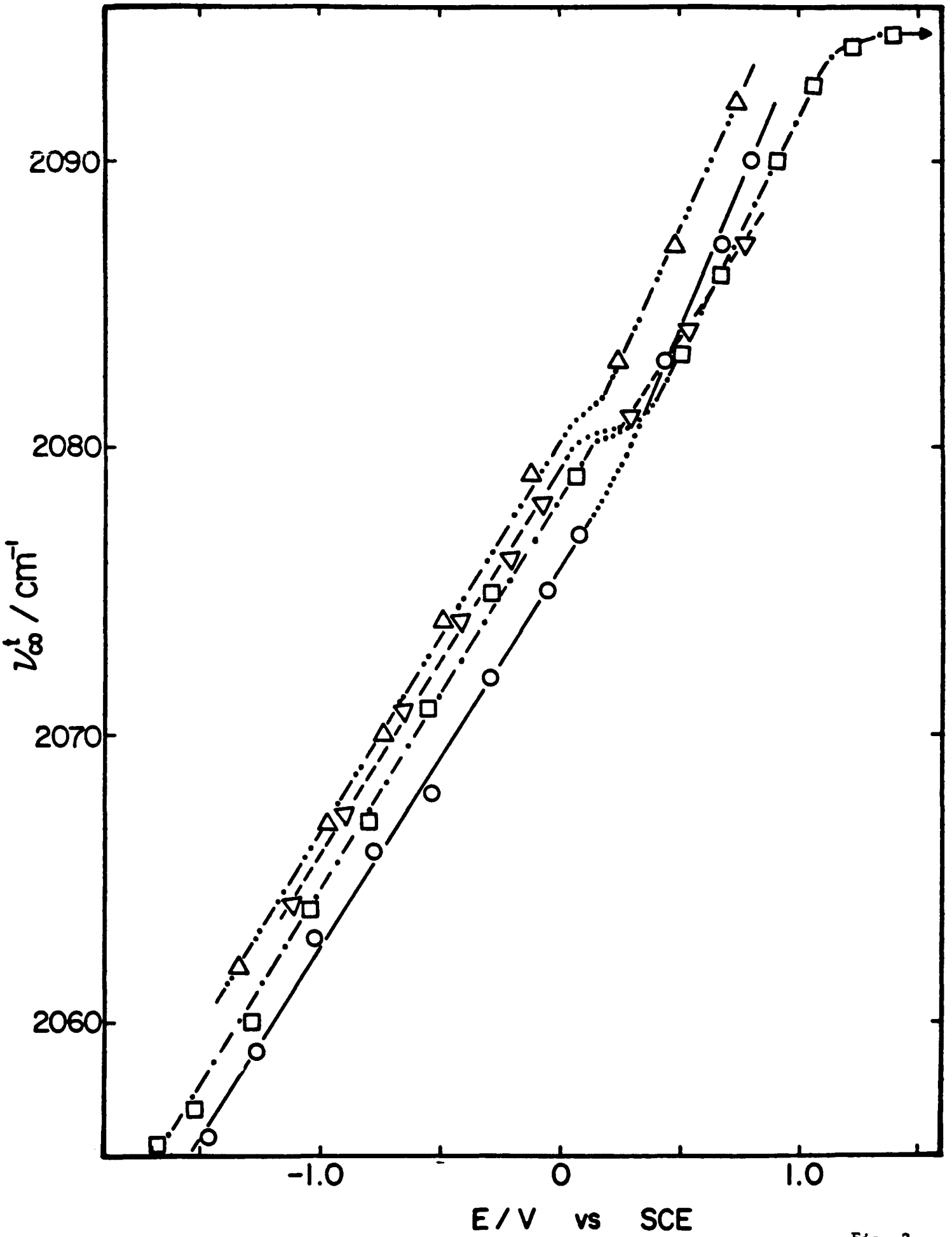

Fig. 2

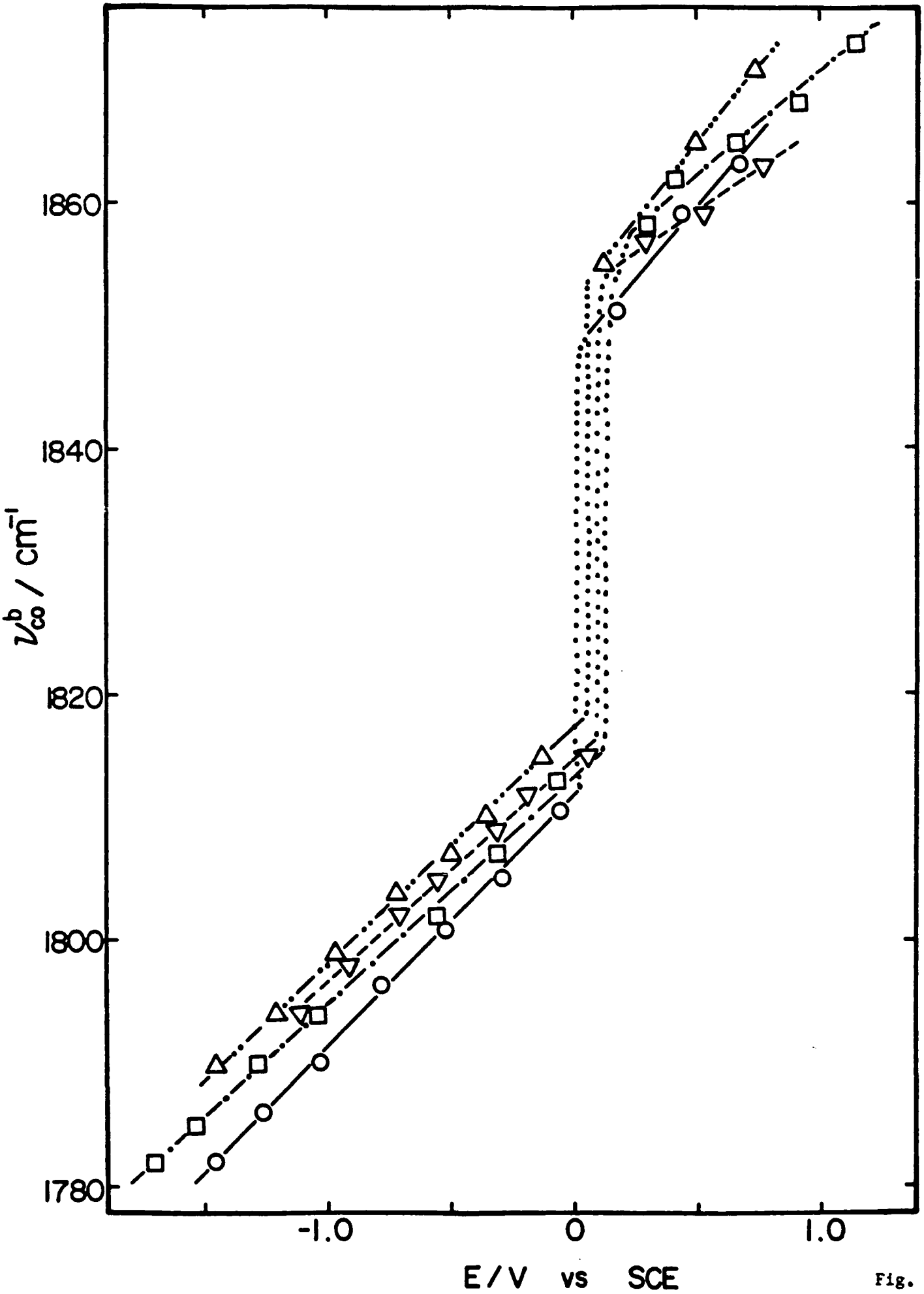

Fig. 3

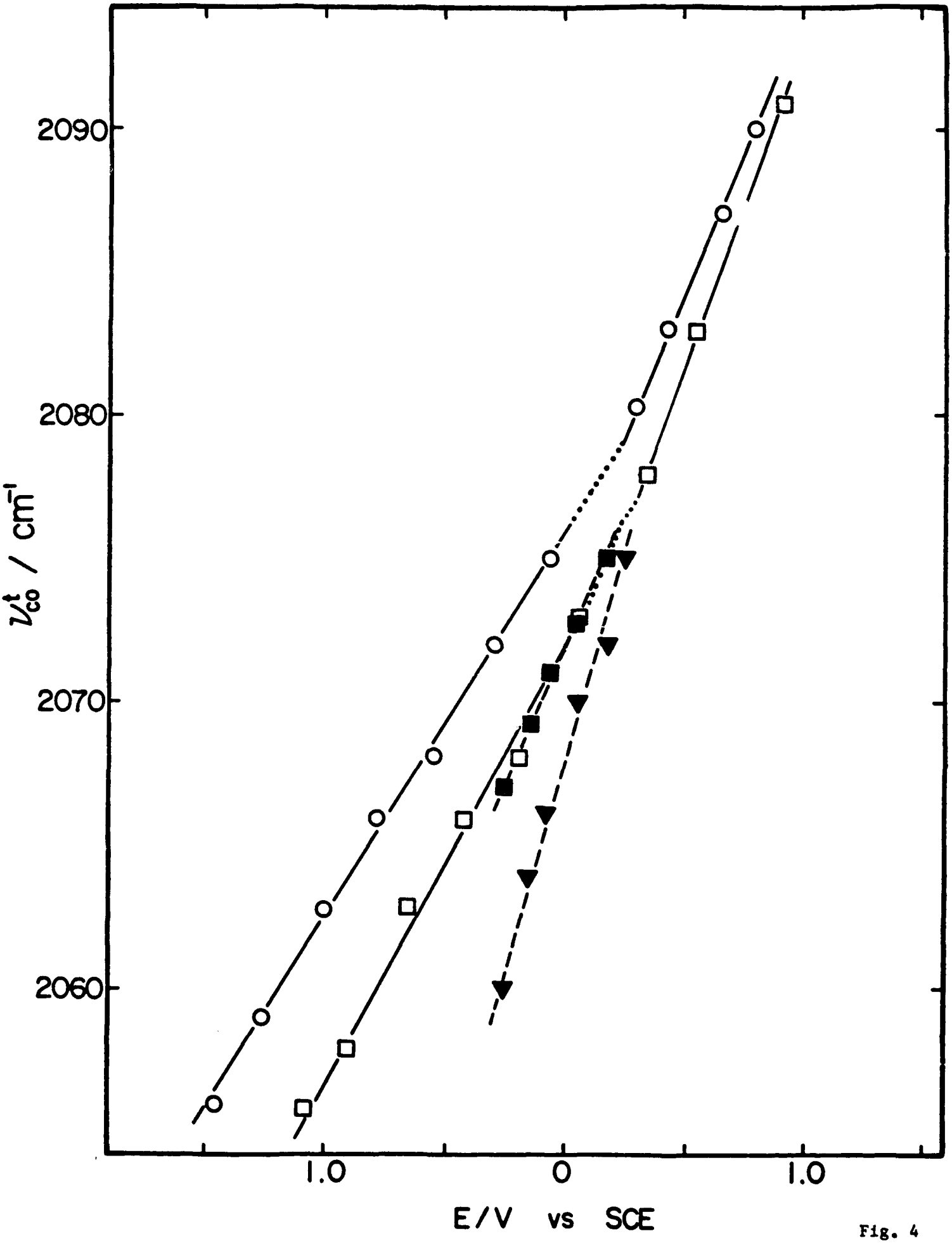

Fig. 4

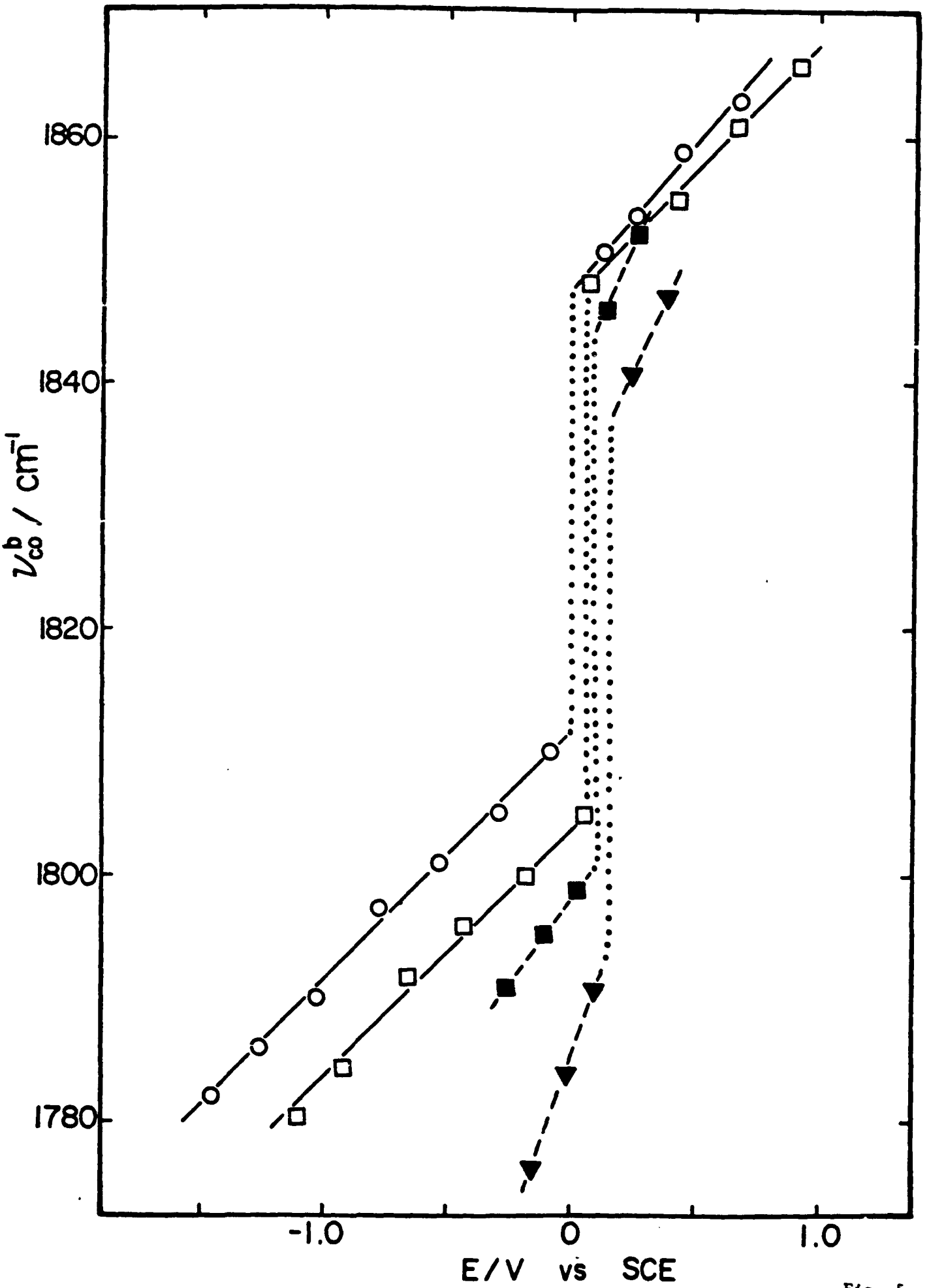

Fig. 5